Cooperative binding of effectors by an allosteric ribozyme

Antony M. Jose, Garrett A. Soukup and Ronald R. Breaker*

Department of Molecular, Cellular and Developmental Biology, KBT 452, Yale University, PO Box 208103, New Haven, CT 06520-8103, USA

ABSTRACT

An allosteric ribozyme that requires two different effectors to induce catalysis was created using modular rational design. This ribozyme construct comprises five conjoined RNA modules that operate in concert as an obligate FMN- and theophylline-dependent molecular switch. When both effectors are present, this 'binary' RNA switch self-cleaves with a rate enhancement of ~300-fold over the rate observed in the absence of effectors. Kinetic and structural studies implicate a switching mechanism wherein FMN binding induces formation of the active ribozyme conformation. However, the binding site for FMN is rendered inactive unless theophylline first binds to its corresponding site and reorganizes the RNA structure. This example of cooperative binding between allosteric effectors reveals a level of structural and functional complexity for RNA that is similar to that observed with allosteric proteins.

INTRODUCTION

Advances in molecular engineering have made possible a more detailed exploration of the catalytic potential of nucleic acids outside the confines of living cells. Ribozymes and deoxyribozymes with more sophisticated catalytic and kinetic characteristics can be created using various molecular engineering strategies, including modular rational design (1,2) and *in vitro* selection methods (3–5). Both approaches have proved useful in creating allosteric ribozymes that function as RNA 'molecular switches' whose catalytic activities can be controlled by specific effector molecules (6,7).

Modular rational design relies on the judicious integration of pre-existing RNA structural elements to create RNA constructs with new characteristics. For example, this approach has been used to create ribozymes that are regulated by binding of ATP (1,8,9) or by binding of oligonucleotides (10–12). In contrast, *in vitro* selection techniques can be used to isolate functional RNA molecules from mutagenized or random sequence populations of molecules. This strategy, employed either alone or in combination with modular rational design, has been used to isolate allosteric ribozymes that respond to effector molecules such as flavin mononucleotide (FMN) (13,14), theophylline (14,15), oligonucleotides (16) and the second messengers cAMP and cGMP (17,18). Moreover, *in vitro* selection has been instrumental in creating new functional RNA elements, such as 'communication modules' (13–15) and allosteric binding sites (17,18), each of which can be used as components for future enzyme engineering efforts.

The architecture and regulatory principles of RNA molecular switches are analogous to those established for their allosteric protein counterparts. Both biopolymers form effector-binding structures that are topographically distinct from the active site of the enzyme (1,19–22). Effector binding to the allosteric site of a polynucleotide or polypeptide enzyme brings about a conformational change that results in an increase or decrease in catalytic rate. Engineered allosteric ribozymes can be highly responsive to specific effector molecules. For example, a Co^{2+}-dependent ribozyme has been created that exhibits ~50 000-fold activation in the presence of 100 μM effector (M.Zivarts, Y.Liu and R.R.Breaker, unpublished results).

Prospective applications of engineered allosteric ribozymes would be somewhat limited if RNA were functionally restricted relative to proteins. Indeed, the performance capabilities of many allosteric proteins include the cooperative binding of effectors and the cooperative assembly of catalytic domains, features that had not been observed in the study of naturally occurring ribozymes or engineered ribozymes. The importance of such cooperative interactions is evident by their widespread utilization by natural proteins (21,22), including, for example, the enzyme aspartate carbamoyltransferase (22) and certain acetylcholine receptors (23). In an effort to broaden the kinetic sophistication exhibited by RNA, we set out to engineer an allosteric ribozyme that demonstrates cooperative effector-binding characteristics. Herein we report the construction of a 'binary' allosteric ribozyme that exhibits cooperativity in binding FMN and theophylline, both of which are required to induce maximum catalytic function.

MATERIALS AND METHODS

Oligonucleotides

Synthetic DNA templates used for *in vitro* transcription were prepared by standard solid phase methods (HHMI Biopolymer/ Keck Foundation Biotechnology Resource Laboratory, Yale University) and were purified by denaturing (8 M urea) PAGE. RNAs were generated by *in vitro* transcription of the appropriate DNA templates that were made double stranded by extension using reverse transcriptase (24). Transcription reactions (100 μl) containing ~250 pmol template DNA, 50 mM

Tris–HCl (pH 7.5 at 23°C), 10 mM $MgCl_2$, 50 mM DTT, 20 mM spermidine, 2 mM each of the four ribonucleoside 5′-triphosphates (NTPs) and 35 U μl^{-1} T7 RNA polymerase were incubated at 37°C for 2 h. The resulting RNA products were purified by denaturing 10% PAGE and isolated from the gel by elution with 10 mM Tris–HCl (pH 7.5 at 23°C), 200 mM NaCl and 1 mM EDTA. The recovered RNA was precipitated with ethanol, resuspended in deionized water and stored at –20°C until use. To produce internally ^{32}P-labeled RNAs, $[\alpha\text{-}^{32}P]UTP$ was added to the transcription reaction. RNAs that were ^{32}P-labeled at the 5′-terminus were generated by first dephosphorylating the 5′-triphosphate moiety of purified transcripts using alkaline phosphatase (Boehringer Mannheim) and then radiolabeling using T4 polynucleotide kinase (New England Biolabs) and $[\gamma\text{-}^{32}P]ATP$, as described previously (25). Labeled RNAs were purified by denaturing 10% PAGE and recovered as described above.

Allosteric ribozyme assays

Internally ^{32}P-labeled TF1 RNA (100–500 nM) was incubated at 23°C in 50 mM Tris–HCl (pH 7.5 at 23°C) and 20 mM $MgCl_2$. Additional reaction parameters, including incubation time and effector concentrations, were as specified for each experiment. Cleavage products were separated by denaturing 10% PAGE and visualized and quantitated using a Molecular Dynamics PhosphorImager and ImageQuant software. Rate constants were derived as described previously (24).

RNA secondary structure probing

The relative incidence of spontaneous transesterification at each phosphodiester linkage of TF1-v1 was established by incubating 5′-^{32}P-labeled RNA for 24 h at 23°C in 50 mM Tris–HCl (pH 8.5 at 23°C), 20 mM $MgCl_2$ and in the absence or presence of various concentrations of effectors. Sequencing ladders generated by treatment with alkali or RNase T1 were prepared as described previously (25). Cleavage products were separated using 10% denaturing PAGE and the relative frequency of spontaneous cleavage at each linkage was determined as described previously (25).

Kinetic framework for a self-cleaving binary switch

To establish a simplified kinetic framework for binary allosteric ribozyme function, three assumptions have been made: (i) the ligand-binding equilibrium is rapidly attained and thus has no influence on the rate of ribozyme cleavage; (ii) the ribozyme is active only when both effectors are bound; (iii) the ribozyme cleavage reaction does not affect the ligand-binding equilibrium (see Supplementary Material). From this framework we obtain an expression (**1**) for the cooperativity coefficient (α) as defined by Ehlert (26), which reflects the extent of binding cooperativity among effectors. The cooperativity coefficient is also equivalent to the ratio of the dissociation constants for FMN departing from the FR complex (K_d^{FR}) to that for FMN departing from the TFR complex (K_d^{TFR}), where T, F and R represent theophylline, FMN and RNA, respectively.

$$\alpha = K_{FT}/K_T = K_{TF}/K_F = K_d^{FR}/K_d^{TFR} \qquad \mathbf{1}$$

An expression for the dependence of the observed rate constant (k_{obs}) on the concentrations of FMN (F) and theophylline (T) is given by **2**, where apparent $V_{max} = (\alpha k K_T[T])/(1 + \alpha K_T[T])$ and

apparent $K_m = (1 + K_T[T])/(K_F + \alpha K_T K_F [T])$ (see Supplementary Material).

$$k_{obs} = (\text{apparent } V_{max} \times [F])/(\text{apparent } K_m + [F]) \qquad \mathbf{2}$$

Equation **2** predicts that for a given concentration of theophylline, the binary allosteric ribozyme exhibits saturation kinetics with respect to FMN concentration. Therefore, the maximum k_{obs} value achievable is limited by the concentration of theophylline, as long as it is non-saturating.

RESULTS AND DISCUSSION

Engineering a binary RNA switch

To further explore the dynamic structural capabilities of RNA, we set out to create a binary self-cleaving ribozyme that requires two distinct effector molecules to induce catalytic function. In addition, we sought a design for the construct that provides for cooperative binding between the two effectors such that binding of one effector controls binding of the other. Successful integration of the latter characteristic would demonstrate that RNA has sufficient structural versatility to form highly responsive enzymatic and genetic switches that are similar in kinetic performance to certain proteins. We chose to employ a modular rational design strategy for ribozyme construction, as this approach has already proved useful for engineering allosteric ribozymes with new effector specificities (1–3,9,13–15).

A ribozyme construct, termed TF1, was assembled using five separate functional RNA modules (Fig. 1A). Module 1 is the hammerhead self-cleaving ribozyme that catalyzes an internal transesterification reaction when incubated in the presence of a divalent metal cofactor such as Mg^{2+} (27). A construct representing the independent module 1 cleaves RNA with a k_{obs} of ~1 min^{-1} under reaction conditions that are similar to those used in this study (1,28). Modules 2 and 3 were derived from a FMN-dependent allosteric ribozyme that was isolated previously using *in vitro* selection. Specifically, module 2 serves as a 'communication module' (cm$^+$FMN1) that precludes full activity of the adjoining ribozyme unless FMN is bound to module 3 (13). The effector-binding RNA comprising module 3 was isolated previously by *in vitro* selection (29). Similarly, modules 4 and 5 were derived from a theophylline-dependent allosteric ribozyme (15) that carries a different ligand-responsive communication module (cm$^+$theo3) and a theophylline-binding RNA aptamer (30), respectively.

With this configuration, the various modules of the TF1 RNA were expected to retain their respective ligand-binding, structure-modulating or catalytic functions. However, each component of TF1 was expected to act in an interdependent fashion to function as a binary switch that exhibits cooperative binding between the theophylline and FMN effectors. Cooperative binding between effectors and subsequent activation of ribozyme function should be modulated by the ligand-dependent formation of four essential base pairing interactions (Fig. 1A, *a–d*). Specifically, the theophylline-binding aptamer is known to be structurally unorganized in the absence of theophylline (25,31), but undergoes 'adaptive binding' (32) of its corresponding ligand by forming a highly ordered RNA–ligand complex (31). Ligand-induced stabilization of the complex includes the formation of interaction *a* (Fig. 1A), which is a
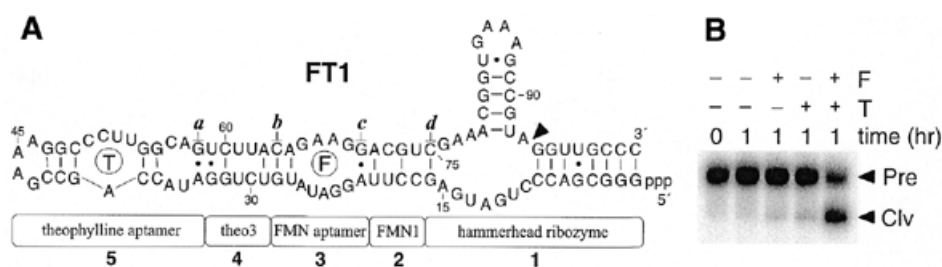
Figure 1. Design and function of a binary RNA switch. (**A**) Modular rational design of TF1 RNA using five distinct RNA modules (numbered 1–5). Individual modules are depicted as an integrated sequence whose boundaries are schematically represented underneath. Communication modules cm⁺theo3 (15) and cm⁺FMN1 (13) are labeled theo3 and FMN1, respectively. Four putative ligand-dependent base pairs are labeled *a*−*d*. An arrowhead denotes the site of ribozyme cleavage. (**B**) Allosteric function of the TF1 RNA. Precursor RNA (Pre, internally ³²P-labeled) was incubated in the absence (−) or presence (+) of 1 mM theophylline (T) and/or 1 mM FMN (F) for 0 or 1 h. The region of gel containing the precursor and the 5′-cleavage fragment (Clv) is shown.

non-canonical G·A base pair located adjacent to cm⁺theo3. The stabilization of base pair *a*, along with neighboring base pairs, is subsequently expected to facilitate the formation of a stem element that includes interaction *b*, which is a canonical G-C pair that is a requisite component of the adjacent FMN-binding aptamer. The formation of this stem-like structure is critical for the function of the theophylline-dependent ribozyme isolated previously (15). Like the theophylline-binding aptamer, the FMN-binding aptamer becomes structurally organized only when FMN is bound. Ligand-induced stabilization of the structure of the FMN aptamer brings about the formation of interaction *c*, which is a non-canonical G·A base pair that is adjacent to cm⁺FMN1. The stabilization of base pair *c*, along with neighboring base pairs, in turn stabilizes interaction *d*, which is a canonical G-C pair whose formation is required for hammerhead ribozyme activity (2,33).

In accordance with the design of the TF1 construct, the ribozyme remains uncleaved in the absence of the two effectors, but exhibits significant self-cleavage activity when incubated in the presence of both theophylline and FMN (Fig. 1B). The rate enhancement for TF1 cleavage in the presence of 1 mM each of the two effectors ($k_{obs} = 1.2 \times 10^{-2}$ min⁻¹) relative to the absence of effectors ($k_{obs} = 4 \times 10^{-5}$ min⁻¹) is ~300-fold. Neither theophylline nor FMN alone can trigger maximal self-cleavage activity. This result is consistent with the design rationale as described above, whereby the ribozyme is rendered inactive until theophylline-mediated stabilization of base pairs *a* and *b* enables FMN binding and its subsequent stabilization of base pairs *c* and *d*.

A related attempt to alter the arrangement of RNA elements in TF1 (Fig. 1A) by exchanging modules 2 and 3 with modules 4 and 5, respectively, failed to produce a functional binary RNA switch (data not shown). Attempts to integrate another aptamer with a different effector specificity to generate a new binary allosteric ribozyme also failed to yield an active construct. Each of these non-functional constructs can adopt secondary structures [predicted using the RNA MFOLD program (RNA MFOLD can be accessed on the internet at http://bioinfo.math.rpi.edu/~mfold)] that differ from that predicted to be critical for molecular switch function. While successful generation of the TF1 binary switch by modular rational design demonstrates the utility of exploiting pre-existing RNA modules for molecular engineering, it is important to note that not all alternative folded states that compete
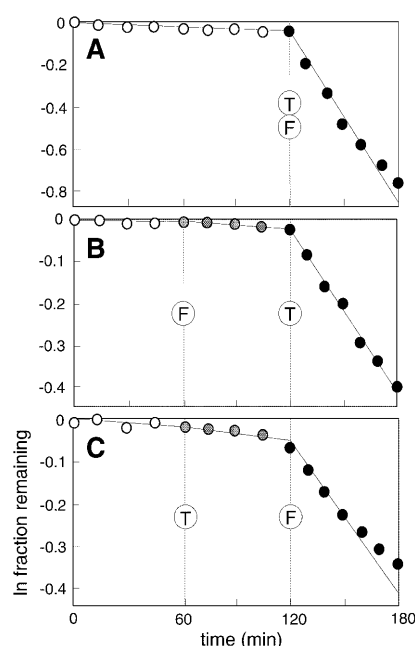
Figure 2. Activation of ribozyme function by two effectors. Plots of the natural logarithm of the fraction of TF1 that remains uncleaved versus time. (**A**) Both FMN (encircled F, 1 mM final concentration) and theophylline (encircled T, 1 mM final concentration) were added simultaneously to a reaction mixture at *t* = 120 min. Similarly, effectors were added independently in (**B**) and (**C**) at *t* = 60 min and *t* = 120 min, as indicated. The fraction of precursor RNAs that self-cleaved were established as described in Materials and Methods.

with individual modules can be anticipated using this engineering strategy.

Specific activation of a binary allosteric ribozyme

A more detailed examination of the allosteric function of TF1 reveals that the ribozyme remains essentially inactive for extended periods of time in the absence of both effectors. However, the RNA readily converts to its active state upon addition of theophylline and FMN (Fig. 2A). This indicates that the inactive structural state(s) adopted by the RNA in the absence of the effectors is dynamic and can be converted to a structure that permits efficient ribozyme function when both effectors are introduced. This structural conversion occurs at a

rate that exceeds the time scale used for the assay. Furthermore, there is only a marginal enhancement of ribozyme activity when either FMN (Fig. 2B) or theophylline (Fig. 2C) is added independently. However, the ribozymes are promptly activated when either reaction is supplemented with the omitted effector, although the k_{obs} value is approximately half that observed when both effectors are added simultaneously. The non-linear nature of the data in Figure 2A indicate that ~25% of the ribozymes might remain misfolded when both effectors are added simultaneously. In addition, the modest reductions in RNA processing rates that are apparent in Figure 2B and C could also be due to partial misfolding of the RNA population, perhaps as a result of extended exposure to only one effector.

Kinetic evidence for positive cooperativity of effector binding

A kinetic framework for proteins that exhibit cooperative binding between ligands has been developed previously (26). Similarly, we have employed a simplified kinetic framework to describe the observed rate constant of TF1 ribozyme cleavage as a function of effector concentration (see Supplementary Material). This framework, depicted in Figure 3A, reflects the various states that the TF1 RNA can assume by forming complexes with either or both of the effector molecules. An expression derived using this framework specifies that when the concentration of the first effector is held constant and k_{obs} is measured at various concentrations of the second effector, the greatest k_{obs} value obtainable is limited by the concentration of the first effector.

To establish the dependence of TF1 ribozyme activity on effector concentrations, k_{obs} values were determined in reactions containing various concentrations of theophylline and FMN (Fig. 3B). The observation that theophylline concentration limits k_{obs} values determined for TF1 at various concentrations of FMN is consistent with the kinetic framework for cooperative binding of effectors. Furthermore, a double reciprocal plot ($1/k_{obs}$ versus $1/[FMN]$) yields a straight line for data generated using fixed concentrations of theophylline and non-saturating concentrations of FMN (Fig. 3C). These data demonstrate that TF1 function exhibits saturation kinetics, as predicted by the kinetic framework for cooperative binding.

The kinetic results depicted in Figure 3 can be rationalized if theophylline binding to TF1 RNA causes a substantial increase in the affinity of the construct for FMN. To explore this possibility, we determined the value for α, the cooperativity coefficient previously defined by Ehlert (26), for effector interaction with TF1. This was achieved by establishing the dissociation constants for FMN interaction with TF1 RNA bound to theophylline (K_d^{TFR}) and FMN interaction with TF1 RNA alone (K_d^{FR}). At high concentrations of theophylline, TF1 RNA is expected to be in complex with theophylline. Therefore, the apparent K_d^{TFR} for FMN can be established by identifying the concentration of FMN needed to achieve half maximal k_{obs} in the presence of saturating (1 mM) theophylline (Fig. 3B and data not shown). Since the maximum k_{obs} for TF1 when saturated with theophylline and FMN is ~1.2×10^{-2} min⁻¹, an apparent K_d^{TFR} for FMN of ~200 μM is obtained. This value is consistent with a dissociation constant previously determined for the parent FMN-dependent ribozyme (13; data not shown). In contrast, the affinity of independent TF1 RNA for FMN in the absence of theophylline is substantially poorer. To provide
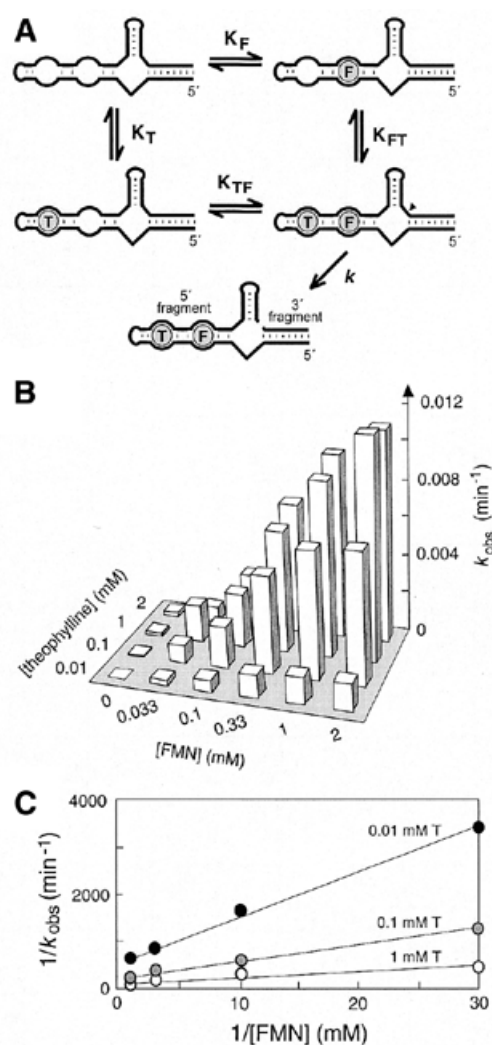

Figure 3. Kinetic modulation of a binary RNA switch. (**A**) Diagrammatic representation of the kinetic framework for binary allosteric ribozyme function. Encircled T and F represent bound theophylline and FMN, respectively. (**B**) Effector-dependent activation of TF1 self-cleavage. The maximum k_{obs} for ribozyme function in 1 mM each of theophylline and FMN is ~1.2×10^{-2} min⁻¹. (**C**) Double reciprocal plots reflecting the dependence of the observed rate constant for TF1 self-cleavage with various concentrations of effectors. Open, shaded and filled symbols represent data collected at 0.01, 0.1 and 1 mM theophylline, respectively.

an estimate of K_d^{FR} we assumed that the maximum k_{obs} for TF1 cleavage is the same upon FMN binding whether or not theophylline is bound (i.e. the FMN binding event is the obligate step for ribozyme activation). Consequently, the apparent K_d^{FR} for FMN is at least 17 mM (data not shown). Therefore, the cooperativity coefficient (K_d^{FR}/K_d^{TFR}), represented by α, is at least 85. Since values for α of >1 reflect positive cooperativity, TF1 function likely involves positive cooperativity in effector binding.

Dynamic reorganization of structure as the basis for cooperative binding

Overall, the kinetic responses exhibited by TF1 are in accordance with the design of the construct, wherein theophylline
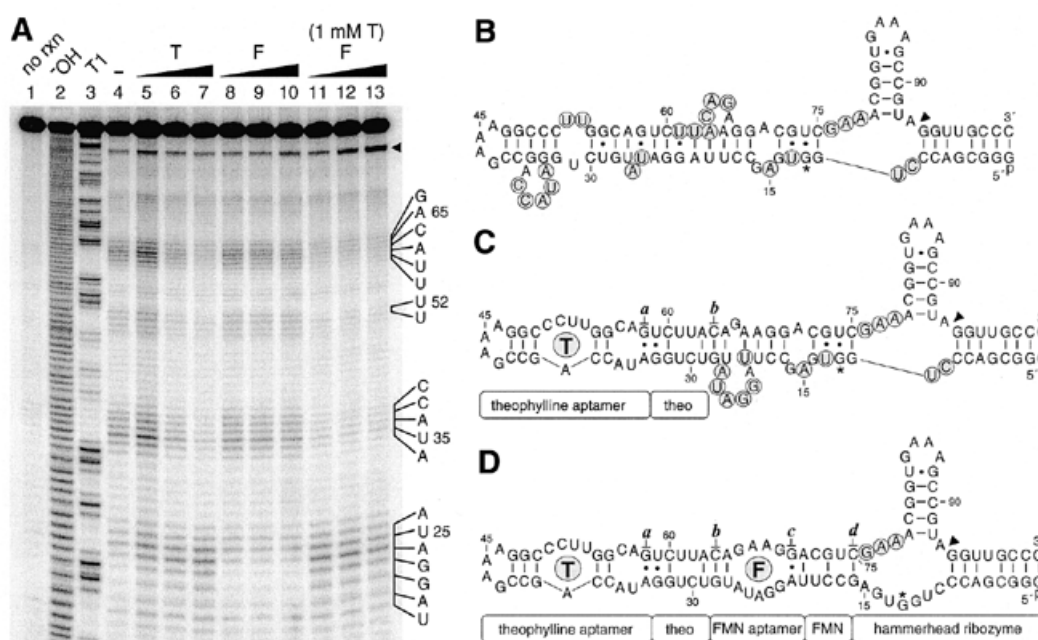
Figure 4. RNA structure probing of various effector–RNA complexes. (**A**) Autoradiogram depicting the distribution of cleavage products resulting from spontaneous transesterification of TF1-v1 RNA. The top-most band represents 5′-^{32}P-labeled TF1-v1 RNA, while lower bands correspond to various 5′-cleavage fragments. Each band reflects spontaneous cleavage at a different site along the polynucleotide chain, which were identified by comparison to TF1-v1 cleavage products generated by partial digestion with alkali (⁻OH) or with ribonuclease T1 (T1). Regions exhibiting the greatest frequency of spontaneous cleavage are denoted by nucleotide sequence and number. RNA strand scission occurs 3′ to each nucleotide listed. The arrowhead identifies the site of ribozyme cleavage. Cleavage products <18 nt in length are not depicted. For reactions grouped in lanes 5–7, 8–10 and 11–13, the three lanes in each contain 0.01, 0.1 and 1 mM, respectively, of the effector indicated. Lanes 11–13 additionally contain 1 mM theophylline. (**B**) Sequence and secondary structure model of TF1-v1 in the absence of effectors. An asterisk denotes the single A→G mutation at position 12 relative to TF1 that was incorporated to reduce ribozyme-mediated RNA cleavage during the probing reaction. Encircled nucleotides identify those positions that exhibit the highest frequencies of spontaneous cleavage under the respective probing conditions. (**C**) Model of TF1-v1 bound to theophylline (encircled T). Labeled rectangles identify RNA modules that are properly folded for binary switch function as depicted in Figure 1A. Other details are as described in (B). (**D**) Model of TF1-v1 bound to theophylline and FMN (encircled F). Other details are as described in (B) and (C).

binding is required for higher affinity binding to FMN and FMN binding is essential for efficient ribozyme function. However, our observations from the kinetic analyses could also in part be explained if the ribozyme required two effectors that do not function cooperatively. In order to obtain direct evidence for cooperative binding, we examined the structures formed by a variant of TF1, termed TF1-v1, by monitoring the spontaneous degradation of RNA in the presence of various effector concentrations and by secondary structure modeling (Fig. 4).

The frequency of spontaneous RNA transesterification is largely dependent on the secondary and tertiary structures that are adopted by the molecule (18,25). Specifically, RNA conformations including stable base paired helices and tertiary structures typically reduce spontaneous RNA cleavage by precluding the transient formation of a labile conformation wherein the 2′-oxygen nucleophile and the 5′-oxyanion leaving group are 'in-line' with respect to the phosphorus center. Therefore, internucleotide linkages that exhibit a high rate of spontaneous cleavage are typically unstructured, while linkages that are relatively resistant to spontaneous cleavage are presumably involved in stable secondary or tertiary structures.

The TF1-v1 RNA used for the probing studies carries a single A→G mutation at position 12 (Fig. 1A) to prevent self-cleavage by the hammerhead ribozyme domain. In the absence of theophylline and FMN, TF1-v1 exhibits significant levels of

spontaneous cleavage at numerous positions along the polynucleotide chain (Fig. 4A, lane 4). For example, the high frequency of RNA cleavage at nucleotides 34–38 and 61–66 are indicative of unfolded regions. Structural heterogeneity within these regions is inconsistent with the secondary and tertiary structures that are predicted to form in the active (effector-bound) state of the TF1 ribozyme (Fig. 1A) or in the independent aptamers (31,32). In contrast, regions that exhibit lower frequencies of spontaneous cleavage in the absence of effectors largely correlate with secondary structures predicted for FT1-v1 using the RNA MFOLD algorithm (Fig. 4B). These data indicate that the nucleotides comprising the FMN-binding aptamer are arranged differently than when conforming to an RNA structure that is known to be readily receptive to FMN binding (25). Therefore, in the absence of theophylline, FMN is predicted to bind to the TF1 RNA with poor affinity due to the occluded structure of its binding site. Furthermore, each of the four base paired elements predicted to be critical for molecular switch function (Fig. 1A, base pairs *a–d*) are lacking in this model.

The pattern of spontaneous RNA cleavage dramatically changes when theophylline is included in the reaction mixture (Fig. 4A, lanes 5–7). At 1 mM theophylline there is a substantial reduction in RNA degradation within regions comprised of nucleotides involved in theophylline binding (e.g. nucleotides 34–38, 51, 52 and 61–66) and there is a simultaneous increase

in spontaneous cleavage in the region comprised of nucleotides 20–26. These data indicate that theophylline binds to its corresponding RNA domain and causes a reorganization of secondary structure throughout the RNA molecule, where nucleotides residing in the otherwise occluded FMN-binding domain are liberated (Fig. 4C). Furthermore, the nucleotides involved in the putative base pair interactions *a* and *b* are shown by the probing experiments to be structured, which is consistent with their involvement in the stem-like form of the cm⁺theo3 element (Fig. 1A).

The pattern of RNA cleavage observed when FMN is included in the reaction mixture remains unchanged from that obtained in the absence of effectors (Fig. 4A, compare lanes 8–10 with lane 4), indicating that FMN alone is incapable of binding and altering the structure of the RNA. In contrast, the frequency of spontaneous cleavage is reduced throughout the molecule when 1 mM theophylline and various concentrations of FMN are included in the reaction mixture (Fig. 4A, lanes 11–13). The most significant changes upon FMN addition relative to the addition of theophylline alone is the ~75% reduction in the frequency of RNA cleavage in the region spanning nucleotides 20–26. This result is consistent with the observation that ~25% of FT1 RNA cleaves with a relatively reduced rate constant when presented with saturating concentrations of theophylline and FMN (data not shown). Presumably, the slower cleaving fraction of RNA fails to adopt an FMN-bound conformation that is compatible with ribozyme function.

The global reduction in spontaneous cleavage of TF1-v1 RNA in the presence of both effectors is congruent with formation of the active secondary structure, including base pairs *a–d*, as depicted in Figure 4D. It is also important to note that although the ribozyme function of TF1-v1 was handicapped by mutation to preclude excessive cleavage during the probing reactions, the rate of cleavage at the ribozyme target site is enhanced when both effectors are added (Fig. 4A, lanes 11–13). This indicates that both TF1 and TF1-v1 undergo similar effector-mediated reorganization of secondary and tertiary structure elements that enable formation of an active ribozyme domain. Therefore, the structure of TF1 in its ligand-stabilized state (Fig. 1A), which is identical to that envisioned for the design of TF1-v1 (Fig. 4D), is expected to be compatible with hammer-head ribozyme function.

CONCLUSIONS

The allosteric ribozyme construct TF1 exhibits negligible activity in the presence of either theophylline or FMN, but exhibits an ~300-fold increase in ribozyme activity when both effectors are present. Structure probing data are consistent with a mechanism for allosteric ribozyme function that involves sequential and cooperative binding of the effectors to the RNA. Specifically, binding of theophylline to TF1 RNA facilitates binding of FMN by inducing an observable conformational change in RNA structure. FMN binding in turn initiates a second structural reorganization that induces activity in the adjoining ribozyme domain. Kinetic studies also indicate that TF1 uses a cooperative binding mechanism to function as a binary RNA switch. The cooperativity coefficient for FMN binding is at least 85, implying that binding of theophylline improves the apparent dissociation constant of FMN by 85-fold or more.

The TF1 allosteric ribozyme was engineered and assembled using a modular rational design strategy wherein five pre-existing RNA modules were joined in a logical fashion to provide the desired activity. However, we expect that constructs generated using a modular rational design strategy will frequently be plagued by unanticipated folding problems. Therefore, a combined approach that employs modular rational design and *in vitro* selection is likely to be the most effective means to construct functional multipartite RNA structures.

The kinetic and structural characteristics of the TF1 construct serve as evidence that RNA is capable of employing more sophisticated regulatory strategies for ribozyme control than had been observed previously. The cooperative binding characteristics exhibited by TF1 are similar to those seen with natural protein receptors and protein enzymes that modulate the binding affinities of ligands or substrates (21,22,26). Cooperativity in allosteric proteins typically results in catalytic function that is tightly controlled by effector concentration, thus providing a narrow range of effector concentration that dictates modulation of protein function. A requisite for proteins that exhibit such sigmoidal or 'digital' kinetic responses to effectors is the cooperative activation of multiple active sites by single effector-binding events, typically involving effector-mediated changes in quaternary structure. Oxygen binding to hemoglobin is a well-studied example of this sigmoidal cooperative modulation of protein function (22). It is likely that RNAs with quaternary structure (11,34) could also be engineered to exhibit digital kinetic profiles in response to effector binding, thereby providing RNA switches that respond sharply to small perturbations in effector concentrations. These RNA constructs would make excellent candidates for applications that require high gain biosensor components or as highly responsive genetic switches.

SUPPLEMENTARY MATERIAL

Supplementary Material is available at NAR Online.

REFERENCES

1. Tang,J. and Breaker,R.R. (1997) Rational design of allosteric ribozymes. *Chem. Biol.*, **4**, 453–459.
2. Soukup,G.A. and Breaker,R.R. (1999) Design of allosteric hammerhead ribozymes activated by ligand-induced structure stabilization. *Structure*, **7**, 783–791.
3. Breaker,R.R. (1997) *In vitro* selection of catalytic polynucleotides. *Chem. Rev.*, **97**, 371–390.
4. Li,Y. and Breaker,R.R. (1999) Deoxyribozymes: new players in the ancient game of biocatalysis. *Curr. Opin. Struct. Biol.*, **9**, 315–323.

5. Wilson,D.S. and Szostak,J.W. (1999) *In vitro* selection of functional nucleic acids. *Annu. Rev. Biochem.*, **68**, 611–647.
6. Soukup,G.A. and Breaker,R.R. (1999) Nucleic acid molecular switches. *Trends Biotechnol.*, **17**, 469–476.
7. Soukup,G.A. and Breaker,R.R. (2000) Allosteric nucleic acid catalysts. *Curr. Opin. Struct. Biol.*, **10**, 318–325.
8. Tang,J. and Breaker,R.R. (1997) Examination of the catalytic fitness of the hammerhead ribozyme by *in vitro* selection. *RNA*, **3**, 914–925.
9. Tang,J. and Breaker,R.R. (1998) Mechanism for allosteric inhibition of an ATP-sensitive ribozyme. *Nucleic Acids Res.*, **26**, 4214–4221.
10. Porta,H. and Lizardi,P.M. (1995) An allosteric hammerhead ribozyme. *Biotechnology*, **13**, 161–164.
11. Kuwabara,T., Warashina,M., Tanabe,T., Tani,K., Asano,S. and Taira,K. (1998) A novel allosterically *trans*-activated ribozyme, the maxizyme, with exceptional specificity *in vitro* and *in vivo*. *Mol. Cell*, **2**, 617–627.
12. Komatsu,Y., Yamashita,S., Kazama,N., Nobuoka,K. and Ohtsuka,E. (2000) Construction of new ribozymes requiring short regulator oligonucleotides as a cofactor. *J. Mol. Biol.*, **299**, 1231–1243.
13. Soukup,G.A. and Breaker,R.R. (1999) Engineering precision RNA molecular switches. *Proc. Natl Acad. Sci. USA*, **96**, 3584–3589.
14. Robertson,M.P. and Ellington,A.D. (2000) Design and optimization of effector-activated ribozyme ligases. *Nucleic Acids Res.*, **28**, 1751–1759.
15. Soukup,G.A., Emilsson,G.A.M. and Breaker,R.R. (2000) Altering molecular recognition of RNA aptamers by allosteric selection. *J. Mol. Biol.*, **298**, 623–632.
16. Robertson,M.P. and Ellington,A.D. (1999) *In vitro* selection of an allosteric ribozyme that transduces analytes to amplicons. *Nat. Biotechnol.*, **17**, 62–66.
17. Koizumi,M., Soukup,G.A., Kerr,J.Q. and Breaker,R.R. (1999) Allosteric selection of ribozymes that respond to the second messengers cGMP and cAMP. *Nature Struct. Biol.*, **6**, 1062–1071.
18. Soukup,G.A., DeRose,E.C. and Breaker,R.R. (2001) Generating new ligand-binding RNAs by affinity maturation and disintegration of allosteric ribozymes. *RNA*, in press.
19. Monod,J. and Jacob,F. (1961) General conclusions: teleonomic mechanisms in cellular metabolism, growth and differentiation. *Cold Spring Harbor Symp. Quant. Biol.*, **26**, 389–401.
20. Monod,J., Changeux,J.-P. and Jacob,F. (1963) Allosteric proteins and cellular control systems. *J. Mol. Biol.*, **6**, 306–329.
21. Kurganov,B.I. (1978) *Allosteric Enzymes*. Wiley, New York, NY.
22. Perutz,M. (1994) *Mechanisms of Cooperativity and Allosteric Regulation in Proteins*. Cambridge University Press, New York, NY.
23. Jakubík,J., Bacáková,L., El-Fakahany,E.E. and Tucek,S. (1997) Positive cooperativity of acetylcholine and other agonists with allosteric ligands on muscarinic acetylcholine receptors. *Mol. Pharmacol.*, **52**, 172–179.
24. Tang,J. and Breaker,R.R. (2000) Structural diversity of self-cleaving ribozymes. *Proc. Natl Acad. Sci. USA*, **97**, 5784–5789.
25. Soukup,G.A. and Breaker,R.R. (1999) Relationship between internucleotide linkage geometry and the stability of RNA. *RNA*, **5**, 1308–1325.
26. Ehlert,F.J. (1988) Estimation of the affinities of allosteric ligands using radioligand binding and pharmacological null methods. *Mol. Pharmacol.*, **33**, 187–194.
27. Symons,R.H. (1992) Small catalytic RNAs. *Annu. Rev. Biochem.*, **61**, 641–671.
28. Fedor,M.J. and Uhlenbeck,O.C. (1992) Kinetics of intermolecular cleavage by hammerhead ribozymes. *Biochemistry*, **31**, 12042–12054.
29. Burgstaller,P. and Famulok,M. (1994) Isolation of RNA aptamers for biological cofactors by *in vitro* selection. *Angew. Chem. Int. Ed. Engl.*, **33**, 1084–1087.
30. Jenison,R.D., Gill,S.C., Pardi,A. and Polisky,B. (1994) High-resolution molecular discrimination by RNA. *Science*, **263**, 1425–1429.
31. Zimmermann,G.R., Jenison,R.D., Wick,C.L., Simorre,J.P. and Pardi,A. (1997) Interlocking structural motifs mediate molecular discrimination by a theophylline-binding RNA. *Nature Struct. Biol.*, **4**, 644–649.
32. Patel,D.J., Suri,A.K., Jiang,F., Jiang,L., Fan,P., Kumar,R.A. and Nonin,S. (1997) Structure, recognition and adaptive binding in RNA aptamer complexes. *J. Mol. Biol.*, **272**, 645–664.
33. Ruffner,D.E., Stormo,G.D. and Uhlenbeck,O.C. (1990) Sequence requirements of the hammerhead RNA self-cleaving reaction. *Biochemistry*, **29**, 10695–10702.
34. Kuwabara,T., Warashina,M., Orita,M., Koseki,S., Ohkawa,J. and Taira,K. (1998) Formation of a catalytically active dimmer by tRNA^{Val}-driven short ribozymes. *Nat. Biotechnol.*, **16**, 961–965.